G Protein β Subunit–null Mutants Are Impaired in Phagocytosis and Chemotaxis Due to Inappropriate Regulation of the Actin Cytoskeleton

Barbara Peracino,* Jane Borleis,‡ Tian Jin,‡ Monika Westphal,§ Jean-Marc Schwartz,§ Lijun Wu,‖ Enrico Bracco,* Günther Gerisch,§ Peter Devreotes,‡ and Salvatore Bozzaro*

*Dipartimento di Scienze Cliniche e Biologiche, Università di Torino, Ospedale S. Luigi, 10043 Orbassano, Italy; ‡Department of Biological Chemistry, Johns Hopkins University School of Medicine, Baltimore, Maryland 21205; §Max-Planck-Institut für Biochemie, 82152 Martinsried, Germany; and ‖Leukosite, Inc., Cambridge, Massachusetts 02142

Abstract. Chemotaxis and phagocytosis are basically similar in cells of the immune system and in *Dictyostelium* amebae. Deletion of the unique G protein β subunit in *D. discoideum* impaired phagocytosis but had little effect on fluid-phase endocytosis, cytokinesis, or random motility. Constitutive expression of wild-type β subunit restored phagocytosis and normal development. Chemoattractants released by cells or bacteria trigger typical transient actin polymerization responses in wild-type cells. In β subunit–null cells, and in a series of β subunit point mutants, these responses were impaired to a degree that correlated with the defect in phagocytosis. Image analysis of green fluorescent protein–actin transfected cells showed that β subunit–null cells were defective in reshaping the actin network into a phagocytic cup, and eventually a phagosome, in response to particle attachment. Our results indicate that signaling through heterotrimeric G proteins is required for regulating the actin cytoskeleton during phagocytic uptake, as previously shown for chemotaxis. Inhibitors of phospholipase C and intracellular Ca^{2+} mobilization inhibited phagocytosis, suggesting the possible involvement of these effectors in the process.

Iɴ chemotaxis, ameboid cells, like leukocytes and *Dictyostelium* cells, respond directionally to chemical gradients; in phagocytosis, they bind and engulf foreign organisms or apoptotic cells (Devreotes and Zigmond, 1988; Rabinovitch, 1995). Chemotaxis and phagocytosis seem to be closely related, suggesting that the underlying signal transduction events and cytoskeletal responses have evolved in parallel (Metchnikoff, 1968). In the simple eukaryote *Dictyostelium discoideum,* and in ameboid cells of the immune systems of animals, chemotactic and phagocytic stimuli elicit a remarkably similar spectrum of behavioral events and biochemical reactions (Devreotes and Zigmond, 1988; Greenberg, 1995). Foremost among these is the polymerization of actin into filaments that support the extension of pseudopods and the formation of phagocytic cups (McRobbie and Newell, 1983; Greenberg, 1995; Zigmond, 1996).

Chemotaxis and phagocytosis involve both G protein–coupled and tyrosine kinase-linked signal transduction pathways. Many chemoattractants interact with serpentine receptors, such as cAMP receptors in *Dictyostelium* and chemokine receptors in leukocytes (Parent and Devreotes, 1996; Murphy, 1996). Agonists for receptor tyrosine kinases trigger actin polymerization and act as chemoattractants (Kundra et al., 1994). With regard to phagocytosis, bound particles activate protein tyrosine kinases, such as *syk,* leading to actin polymerization and rearrangement, possibly through involvement of the small G protein Rho (Greenberg et al., 1994, 1996; Indik et al., 1995; Hackam et al., 1997). Heterotrimeric G proteins have been involved in chemotactic activation of macrophages, which leads to phagocytosis (Thelen and Wirthmueller, 1994), and in phagosome-endosome fusion (Desjardins et al., 1994; Béron et al., 1995; Allen and Aderem, 1996), whereas no compelling evidence has been reported so far for a role of G proteins in phagocytic uptake.

D. discoideum amebae contain a single G protein β subunit; its deletion creates cells that lack functional G proteins (Lilly et al., 1993; Wu et al., 1995). These mutants are severely defective in chemotaxis, aggregation, and development. When plated on bacterial lawns, they form smooth plaques consisting of monolayers of undifferentiated cells. These plaques are much smaller than those of wild type (Wu et al., 1995). We report here that this slow growth reflects a severe defect in phagocytosis, which is primarily

due to a failure in organizing the actin meshwork into a phagocytic cup. We have also used several inhibitors of G protein–linked effectors, such as protein kinase A (PKA),[1] protein kinase C (PKC), and phospholipase C (PLC) tyrosine kinases, phosphoinositide 3-kinase (PI3) and phosphoinositide 4-kinase (PI4), as well as signal transduction mutants, to dissect the downstream components involved in phagocytosis. We suggest that a signaling pathway mediated by heterotrimeric G proteins, possibly involving PLC activation and mobilization of Ca^{2+} ions, is necessary to regulate the actin cytoskeleton during phagocytosis.

Materials and Methods

Cell Cultures

The following *D. discoideum* strains were used throughout: wild-type strains AX2 and AX3; β subunit–null strains LW6 and LW14, or β subunit point mutants S1, S2, S3, I1, I2; "rescue" mutants LW18 and LW20. Transformation, selection, and developmental phenotype of the mutants have been described by Lilly et al. (1993) and Wu et al. (1995).

For axenic growth, cells were cultured in AX2 medium (Watts and Ashwort, 1972) under shaking at 150 rpm and 23°C. G418 at a concentration of 20 μg/ml was added to cultures of LW14, point mutants, LW18, and LW20. For starvation, cells were washed twice in 0.017 M Na-K Soerensen phosphate buffer, pH 6.0, and then shaken in the same buffer at a concentration of 10^7 per ml.

Phagocytosis Microassays

Phagocytosis was measured by a modification of a previously described assay (Bozzaro et al., 1987), using cells starved for 30 min. Cells were vortexed and mixed with cold FITC-labeled *Escherichia coli* B/r, or in some cases *Salmonella minnesota R595,* at a final concentration of 4×10^6 cells and 5×10^9 bacteria per ml, respectively, in a final volume of 0.1 ml in 5-ml polystyrene tubes. The tubes were placed on a rack mounted on a vortex equipped with speed control (model Reax 2000; Heidolph, Kelheim, Germany), and shaken at 200 vibrations per minute. At various time points, cells were washed free of unbound bacteria by dilution with 5 ml of cold 0.050 M Na-phosphate buffer, pH 9.2, and centrifugation at 110 *g* for 3 min. After additional washing, the cell pellet was resuspended in 1 ml of Na-phosphate buffer containing 0.2% Triton X-100 and then lysed for 30 min. Fluorescence in cell lysates was measured in a spectrofluorimeter (model SFM25; Kontron, Schlieren, Switzerland) at an excitation wavelength of 470 nm and emission of 520 nm. To determine the number of bacteria, a calibration curve was made by serial dilutions of FITC-labeled bacteria lysed with 1% SDS for 2 min at 90°C (Vogel, 1987).

For measuring phagocytosis of latex beads, cells at a final concentration of 4×10^6 per ml were mixed with a suspension of 1-μm-diam standard Dow latex beads (Serva, Heidelberg, Germany) at a final OD of 1.5, in a total volume of 0.1 ml Soerensen phosphate buffer. At the end of incubation, cells were washed free of beads by dilution and washing as above. The cell pellet was resuspended in 1-ml Soerensen phosphate buffer containing Triton X-100, lysed, and then the OD of the suspension was measured. The percentage of engulfed beads was determined by reference to a serial dilution curve of latex beads.

Phagocytosis of yeasts was studied under similar conditions, by mixing 2×10^6 cells per ml with a fivefold excess of TRITC-labeled, heat-killed yeast particles. At the end of the incubation, 0.9 ml of cold Soerensen phosphate buffer was added to each sample, followed by the addition of 0.1 ml of trypan blue (2 mg/ml in 0.02 M citrate buffer containing 0.15 M NaCl) for quenching the fluorescence of noningested particles (Hed, 1986; Maniak et al., 1995). After 15 min of incubation under shaking, excess trypan blue was removed by centrifugation and washing, and then fluorescence determined at 544/577 nm in the spectrofluorimeter.

FITC bacteria were freshly prepared by incubating the bacteria at a final concentration of 10^{10}/ml with 0.1 mg/ml FITC (Sigma Chemical Co., St. Louis, MO) as described (Vogel, 1987), except that the incubation time and temperature were 90 min and 23°C. TRITC yeasts were prepared by labeling 2×10^{10} heat-killed yeast particles in 20 ml of 0.05 M Na$_2$HPO$_4$, pH 9.2, containing 2 mg/ml TRITC (Sigma Chemical Co.) and incubating at 37°C for 30 min under shaking. After extensive washing, the TRITC yeasts were aliquoted in 0.017 M Na-K Soerensen phosphate buffer, pH 6.0, and stored at −20°C until use.

Growth Assays on Bacteria or Axenic Medium

For measuring growth on shaken bacteria, cells were inoculated at 5×10^4 per ml in a suspension of 10^{10} *E. coli* B/r per ml, and cell number was counted every 3 h for a total of 36 h. Colony growth on bacterial lawns was assessed by inoculating cells with a toothpick on a lawn of *E.coli* B/2 cultivated on nutrient agar and then measuring the diameter of the plaque every 12 h for a total of 48 h.

For growth in axenic medium, growing cells were diluted to 10^5 per ml in fresh axenic medium and counted every 8 h for a total of 56 h.

Fluid-Phase Endocytosis Assay

Fluid-phase endocytosis was measured as described by Aubry et al. (1993) using FITC-labeled dextran (70,000; Sigma Chemical Co.) as a marker, except that the final volume was 0.1 ml per time point.

Actin Polymerization Assay

Chemoattractant-induced F-actin formation was measured as described (Hall et al., 1988). Briefly, cells were shaken at 2×10^7/ml in Soerensen phosphate buffer. At various time points after addition of 10^{-6} M cAMP or supernatant from bacterial growth medium, 0.1-ml cell suspension was transferred to 0.9-ml stop solution containing 3.7% formaldehyde, 0.1% Triton X-100, 0.25 μM TRITC-phalloidin in 20 mM K-PO$_4$, 10 mM Pipes, 5 mM EGTA, 2 mM MgCl$_2$, pH 6.8. After staining for 1 h, samples were centrifuged for 5 min in a microfuge (model Biofuge A; Heraeus, Hanau, Germany), pellets were extracted with 1 ml methanol for 20 h, and then fluorescence (540/575 nm) was read in a spectrofluorimeter. Bacteria-conditioned medium was prepared by clarification of a stationary phase culture of *Klebsiella aerogenes* grown at 22°C. Medium was used as a stimulus at a dilution of 1:100.

Transfection with Green Fluorescent Protein–Actin

Fusion of the coding region of the *D. discoideum* actin with the red-shifted green fluorescent protein (GFP) S65T mutant has been described (Westphal et al., 1997). Two vectors for expression of the GFP–actin fusion were constructed, one in which the fusion product was inserted in the pDEX H vector containing the resistance to G418 (Faix et al., 1992), and a second based on the pBsr2 vector containing the resistance to blasticidin (Sutoh, 1993). The first vector was used for transforming AX2, AX3, and LW6, and the second vector for LW20, which is already resistant to G418. Transformation was done by electroporation and transformants were selected on plates in nutrient medium containing 20 μg/ml G418 or 10 μg/ml blasticidin. Individual clones were used in the experiments.

Light and Fluorescence Microscopy of Living and Fixed Cells

Phagocytosis of yeast particles by single cells incubated on Petriperm dishes (no. 26136906; Heraeus) was followed for 2 h by time-lapse videomicroscopy using an Axiovert microscope (model 35; Carl Zeiss, Inc., Oberkochen, Germany) equipped with a 100× Neofluar objective and a Zeiss charge-coupled device videocamera (model ZVS-47DE) connected to a Panasonic videorecorder (model 6050; Osaka, Japan). Images were recorded at an interval of 0.5 s.

Cells incubated with TRITC-labeled yeast particles on glass coverslips were fixed with picric acid and formaldehyde and postfixed with 70% ethanol as described by Humbel and Biegelmann (1992). The fixed cells were labeled with 0.5 μg/ml FITC-phalloidin (Sigma Chemical Co.) for 30 min at room temperature, and confocal sections taken on an inverted Zeiss microscope (model LSM 410) with a 100× Neofluar 1.3 oil-immersion objective. For excitation, the 488-nm band of an argon-ion laser line was used and its emission collected with a 510–525-nm bandpass filter for FITC and a longpass filter of 570 nm for TRITC.

---

1. *Abbreviations used in this paper*: gβ⁻, Gβ-null mutants; GFP–actin, green fluorescent protein–actin fusion protein; PLA2, phospholipase A2; PLC, phospholipase C; PKA, protein kinase A; PKC, protein kinase C; PI3 kinase, phosphoinositide 3-kinase; PI4 kinase, phosphoinositide 4-kinase.

Confocal serial images of living cells expressing GFP–actin and incubated with TRITC-labeled yeast particles on glass coverslips were obtained by scanning at intervals of 34 s, using a 100× Plan-Neofluar objective. To avoid damaging the cells upon intense light exposure, the laser intensity was attenuated to 1/100 of its maximal power. Since the yeast particles were strongly labeled, the small fraction of their emission obtained by excitation as 448 nm was sufficient to record their fluorescence together with that of GFP. The two contributions to the emission signal could be separated by using a bandpass filter of 510–525 nm for GFP and a longpass filter of 570 nm for TRITC. Phase contrast was recorded simultaneously. The images from the green channel in Fig. 7 were pseudocolored with a color code ranging from cyan to yellow, and then superimposed to the red channel using Applied Visualization Systems (Waltham, PA) software.

Nuclei of cells growing in axenic medium were labeled with 4′,6-diamidino-2-phenylindole (Sigma Chemical Co.) after cell fixation and postfixation as above. The number of nuclei per cell was determined on a Leitz fluorescence microscope (model Laborlox D; Wetzlar, Germany) using a LH102Z filter.

Results

Phagocytosis and Growth on Bacteria Are Impaired in β Subunit–null cells and Restored in Rescue Mutants

Phagocytosis was assessed in wild-type and in β subunit–null ($g\beta^-$) cells by measuring the uptake rate of fluorescently-labeled *E. coli* B/r or latex beads. Shaken wild-type cells engulfed ~300 bacteria per hour under our conditions, a value in the range of previously published data (Gerisch, 1959; Vogel et al., 1980; Bozzaro et al., 1987). In cells lacking the G protein β subunit, the initial uptake rate of bacteria or latex beads was decreased to 20 or 40–60% of the wild-type rate, respectively (Fig. 1, *A* and *B*). Constitutive expression of wild-type β subunit cDNA in $g\beta^-$ cells restored nearly normal rates of phagocytosis (Fig. 1, *A* and *B*). Replacing *E. coli* B/r with *Salmonella minnesota R595,* which is known to adhere stronger to the surface of *Dictyostelium* cells (Malchow et al., 1967; Bozzaro and Gerisch, 1978; Niewöhner et al., 1997), did not significantly alter the uptake rates of β subunit–null mutants, rescue mutants, or wild-type cells (data not shown). It is open to what extent uptake of different types of bacteria, or of inert particles, such as latex beads, is mediated by different receptors in *Dictyostelium*, though some genetic evidence favors the hypothesis that both specific, lectin-type receptors and non-specific receptors contribute to phagocytosis (Vogel et al., 1980; Bozzaro and Ponte, 1995; Chia, 1996). The defect in phagocytosis of $g\beta^-$ cells seems, however, to be independent of particle binding to a particular receptor, since the uptake of *E.coli*, *S. minnesota R595* as well as latex beads was inhibited in the mutant and restored in rescue cells.

We measured growth of $g\beta^-$ and rescue cells both in shaken suspension or on a lawn of *E. coli.* Consistent with the phagocytosis defect, the doubling time on shaken suspensions was increased from 3 to 10 h in $g\beta^-$ cells and the rate of plaque expansion on bacterial lawns was decreased from 0.6 to 0.1 mm/h. Normal rates of growth under both conditions were found for the rescue cells (Table I).

We also examined individual clones expressing different randomly mutagenized β subunit cDNAs. None of the mutant proteins rescued the developmental defects of the $g\beta^-$ cells; the individual clones all formed smooth plaques. Rates of phagocytosis and doubling times in suspensions of *E. coli* closely correlated with their plaque sizes (Table I), presumably depending on the severity of the mutation.
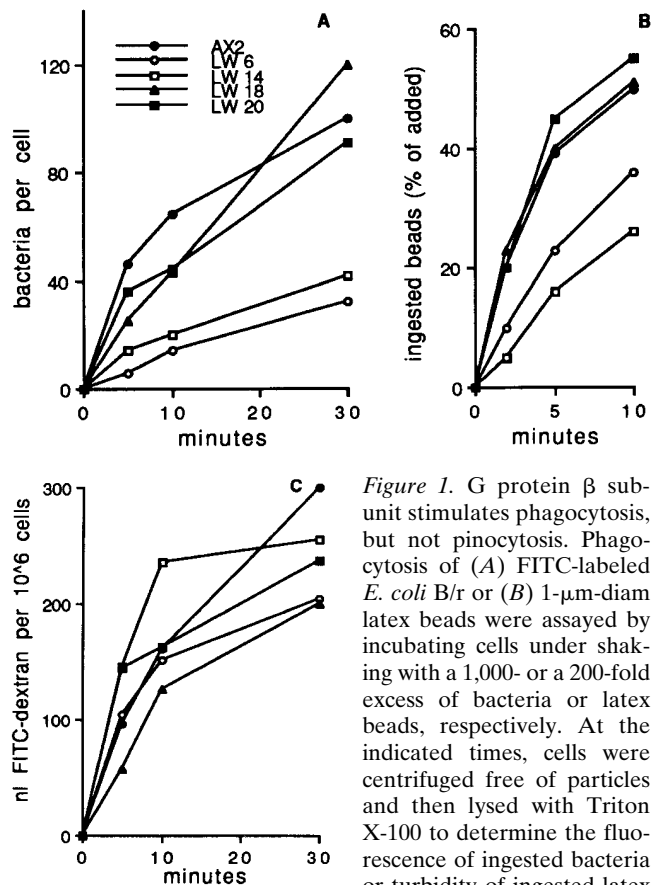

Figure 1. G protein β subunit stimulates phagocytosis, but not pinocytosis. Phagocytosis of (*A*) FITC-labeled *E. coli* B/r or (*B*) 1-μm-diam latex beads were assayed by incubating cells under shaking with a 1,000- or a 200-fold excess of bacteria or latex beads, respectively. At the indicated times, cells were centrifuged free of particles and then lysed with Triton X-100 to determine the fluorescence of ingested bacteria or turbidity of ingested latex beads. (*C*) Pinocytosis of FITC-labeled dextran dissolved in axenic medium was tested under similar conditions. In both cases, 30-min starving cells are used. *AX2,* wild-type; *LW 6* and *LW 14,* gβ⁻clones; *LW 18* and *LW 20,* rescue clones. Results are the average of duplicate determinations in parallel experiments performed with the same cell culture. SD varied between ±4 and 20% of the values shown. Similar results were obtained in a total of (*A*) six, (*B*) five, and (*C*) two independent experiments, respectively. For further details, refer to Materials and Methods.

The diameters of these plaques were small like those of the $g\beta^-$ cells, intermediate, or large like those of rescued mutants (Table I).

Pinocytosis, Cytokinesis, and Motility Are Normal in β Subunit–null Cells

Although the $g\beta^-$ cells were severely defective in chemotaxis and phagocytosis, they were competent in cytokinesis, pinocytosis, and random motility. Pinocytosis was directly monitored by measuring uptake of FITC-conjugated dextran. The initial rates of uptake were essentially identical in mutant, wild-type, and rescued cells (Fig. 1 *C*). Doubling times and cytokinesis of $g\beta^-$ and wild-type cells in liquid media were also similar (Table I). We also monitored the random motility of undifferentiated cells on hydrophilic Petriperm surfaces and found that it was 3.9 (±1.6 SD) and 3.6 (±1.8 SD) μm/min for wild-type and $g\beta^-$cells, respectively. Finally, no differences in cell adhesion to polystyrene surface were detected between undifferentiated $g\beta^-$ and control cells (data not shown). Taken

Table I. Correlation between Chemoattractant-induced F Actin Assembly, Phagocytosis, and Growth on Bacteria

Strain	Doubling in medium	Cytokinesis (*nuclei/cell*)	Plaque growth	Doubling in shaken *E. coli*	Phagocytosis rate (% of WT)	F actin formation (% of WT)
	(*h*)		(*μm/h*)	(*h*)		
AX2	8	1.18 ± 0.02	0.60	3	100	100
LW6	8	1.32 ± 0.13	0.09	10	21	<10
LW14	8	NT	0.11	10	29	<10
LW18	8	1.22 ± 0.08	0.45	3	70	90
LW20	8	1.21 ±0.03	0.40	4	70	85
S1	8	NT	0.39	6	67	59
I1	8	NT	0.09	10	25	17
I2	8	NT	0.10	10	33	14
S2	8	NT	0.25	6	40	48
S3	8	NT	0.47	4.5	70	43

WT (*AX2*), $g\beta^-$ (*LW6* and *LW14*), "rescue" (*LW18* and *LW20*) and β-subunit point mutants (*S1* to *S3*) were tested for growth (column 2) and cytokinesis (column 3) in axenic medium, growth on a lawn of *E. coli* B/2 (column 4) or in shaken cultures of *E. coli* B/r (column 5). Percentage inhibition of phagocytosis rate after 10 min incubation with FITC-*E. coli* B/r is shown in column 6. Percentage actin polymerization in response to chemoattractants present in bacterial supernatants was measured per each strain as described in Fig. 2, and shown in column 7. *NT*, not tested. The values shown are mean values of: two experiments (column 2), 100–150 cells per clone (column 3), three experiments for a total of six plaques per clone (column 4), two experiments for a total of four cultures (column 5), six (*AX2* to *LW20*) and two (*S1* to *S3*) duplicate determinations (column 6), two experiments in triplicates. For details refer to Materials and Methods.

together, these results strongly indicate that the small plaque size of $g\beta^-$ cells on bacterial lawns is solely due to a defect in phagocytosis and not to additional defects in cytokinesis or motility.

The Phagocytosis Defect Is Correlated with Impaired F-actin Formation in Response to Chemoattractants

Chemoattractants induce rapid, transient increases in cellular levels of filamentous actin (McRobbie and Newell, 1983; Hall et al., 1988; Tardif et al., 1995). As previously reported, $g\beta^-$ cells are not attracted to folic acid, cAMP, or bacteria-conditioned medium containing a broad range of chemoattractants. Overexpression of the surface receptor cAR1 does not restore sensitivity to cAMP (Lilly et al., 1993). Consistent with these results, the actin polymerization responses triggered by these compounds are undetectable in $g\beta^-$ cells (Fig. 2). We also examined the series of β subunit point mutants for actin polymerization elicited by bacteria-conditioned medium or cAMP. The magnitudes of these responses correlated with the rates of phagocytosis as well as growth rates on shaken suspensions or lawns of bacteria (Table I; Fig. 3 and data not shown).

The β Subunit–null Cells Are Defective in Reshaping the Actin Cytoskeleton into a Phagocytic Cup

The correlation between actin polymerization and bacteria uptake prompted us to examine actin localization during phagocytosis in $g\beta^-$ cells. Labeling with phalloidin or anti-actin mAbs failed to reveal major differences in actin distribution between $g\beta^-$, rescue, or wild-type cells incubated with bacteria (data not shown). Consistent with the reduced uptake rates of particles, $g\beta^-$ cells contained fewer bacteria in their cytoplasm, some of which were surrounded by actin, probably representing freshly ingested phagosomes.
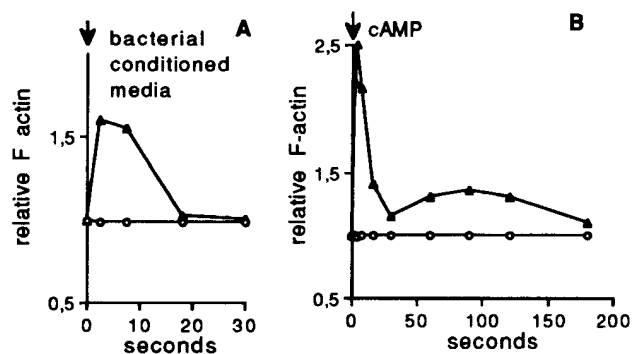
Figure 2. G protein β subunit is required for chemoattractant-induced actin polymerization. F-actin formation in suspended cell cultures following addition of: (*A*) supernatants from bacterial growth medium or (*B*) 10^{-6} M cAMP. *Closed triangles*, LW20; *open circles*, LW6. (*A*) 1- or (*B*) 4-h starving cells were used. The mean value of triplicate determinations is shown. Similar results were obtained in five independent experiments. For experimental details refer to Materials and Methods. Bacterial-conditioned medium was prepared by clarification of a stationary phase culture of *K. aerogenes* grown at 22°C. Medium was used as a stimulus at a dilution of 1:100.

To recognize details, we replaced bacteria by the larger heat-killed yeasts. Like uptake of bacteria, engulfment of suspended yeast was strongly inhibited in the mutant (Fig. 4). Yeast uptake by cells incubated on a hydrophilic Petriperm surface was recorded. In parallel, cells were fixed at different times and labeled with FITC-phalloidin. A serial image sequence of individual wild-type or $g\beta^-$ cells incubated with yeast particles is shown in Fig. 5. Both cell types extended leading edges, and bound yeast particles, which they came in contact with, without detectable differences. Binding either led to formation of a phagocytic cup around a particle or was followed by detachment. Similarly, when a phagocytic cup was formed, the cup could progress up to engulfment of the particle or a new leading front was formed, with subsequent cell detachment from the yeast particle. This behavior is consistent with a zipper model of phagocytosis (Swanson and Baer, 1995), which has been shown to apply to *Dictyostelium* (Maniak et al., 1995). All these events occurred in wild-type and $g\beta^-$ cells, but with significantly different probabilities. As shown in Table II, the number of yeast–cell attachment events leading to successful phagocytic cup formation and engulfment was strongly reduced in $g\beta^-$ cells. The mutant was defective in both steps, phagocytic cup, and phagosome formation, with an inhibition of 35 and 80%, respectively, compared
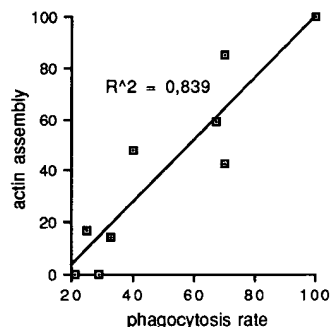
Figure 3. Phagocytosis correlates with rates of F-actin formation in response to chemoattractants. The data reported in Table I, columns 6 and 7 for $g\beta^-$ cells, point mutants, rescue cells, and wild-type were plotted to determine the regression curve (R^{-2}).
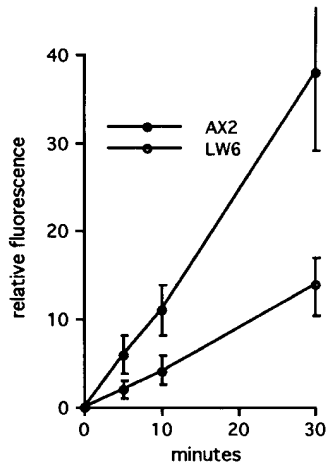
Figure 4. G protein β subunit mutants are impaired in yeast particle uptake. Phagocytosis of TRITC-labeled heat-killed yeast particles by AX2 (*closed circle*) or LW6 (*open circle*) was measured by incubating cells with a fivefold excess of particles for the indicated times. At the end of the incubation, the cells were diluted 10-fold with cold buffer containing trypan blue for quenching the fluorescence of noningested particles. The fluorescence of ingested yeasts was determined in a spectrofluorimeter as described in Materials and Methods. Mean values of three duplicate experiments ±SD are shown.

Table II. Quantitation of Phagocytic Cup and Phagosome Formation in Wild-Type and gβ⁻ Cells Incubated with Yeast Particles

Strain	(I) Adhesion events	(II) Cup formation	Success rate (II/I)	(III) Engulfment	Success rate (III/I)
			(%)		(%)
WT	115	90	78	56	48
$g\beta^-$	252	152*	60	22‡	9

Adhesion events, cells and particles in close contact; *phagocytic cup formation*, half cup formed around a particle; *engulfment*, particle surrounded by the plasma membrane. The number of observed events is shown and the success rate calculated as percentage of successful phagocytic cup formation (*II/I*) or engulfment (*III/I*) in total adhesion events. Experimental conditions are as in Fig. 5. Values are from two experiments for WT and four for LW6. *, $P = 0.0012$; ‡$P < 0.0001$ relative to WT (Chi-test).

with wild-type cells. However, no qualitative differences in phalloidin labeling between wild-type and mutant cells could be detected in fixed parallel samples; the cell cortex of both control and $g\beta^-$ cells was decorated with actin, as were phagocytic cups and freshly ingested phagosomes (Fig. 6).

To follow the dynamics of actin assembly during phagocytosis in individual cells, actin was tagged with GFP (Westphal et al., 1997). Serial image analysis of GFP–actin-producing cells showed that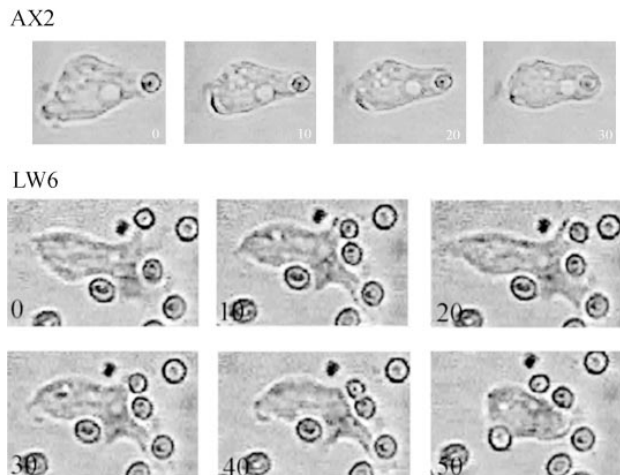 $g\beta^-$ cells, similarly to the other cell lines (AX2, AX3, and LW20), formed leading edges, in which actin was enriched, and often switched from one front to another, to which actin was newly recruited (Fig. 7). Thus, β subunit–null cells are not defective in rapid, spontaneous accumulation of actin at leading edges or other sites of the membrane. We monitored several events of cell–yeast particle adhesion to determine whether adhesion resulted in local actin recruitment and whether the local actin meshwork was converted into a phagocytic cup with the same probabilities in wild-type and $g\beta^-$ cells. As shown in Table III, actin was found to accumulate at sites of cell–yeast particle adhesion in ~50% of the cases in both wild-type and $g\beta^-$ cells. These data are consistent with the hypothesis that particle binding does not automatically trigger actin recruitment, though the low number of cases observed might have obscured differences between wild-type and mutant cells. However, independently of whether or not binding stimulates actin recruitment, the ratio of particle engulfment versus events in which actin was enriched at sites of cell–yeast adhesion was found to be significantly reduced in the mutant (Table III). In most cases no phagocytic cup, and in a few cases only a half cup was formed, followed by actin dissociation from the adhesion site after 30–90 s (Fig. 7, *D* and *E*). It is worth mentioning that this was usually a sufficient time interval for successful phagosome formation, both in the wild-type and in the mutant. Fig. 7 *E* further shows that particles can attach to the surface of mutant cells for a much longer time period. Thus, $g\beta^-$ cells seem to be impaired in reshaping the actin cytoskeleton at adhesion sites into a phagocytic cup and eventually a phagosome. We never observed, neither in wild-type nor in the mutant, successful uptake in the absence of locally enriched actin.

Downstream Transduction Pathways Regulating Phagocytosis

In a preliminary attempt to dissect the cascade of signal transduction that leads from the G protein to phagocytic uptake, we tested the effects of several inhibitors on phagocytosis. Most of the drugs interfere with main effectors linked to G protein, such as PKA, PLC, and PKC, or with influx or intracellular mobilization of Ca^{2+} ions. Table IV summarizes the results obtained with these drugs as well as phospholipase A2 (PLA2), tyrosine kinase, and PI3/PI4 kinase inhibitors. Phagocytosis was strongly affected by PLC inhibitors, such as U73122 and manoalide, and by the
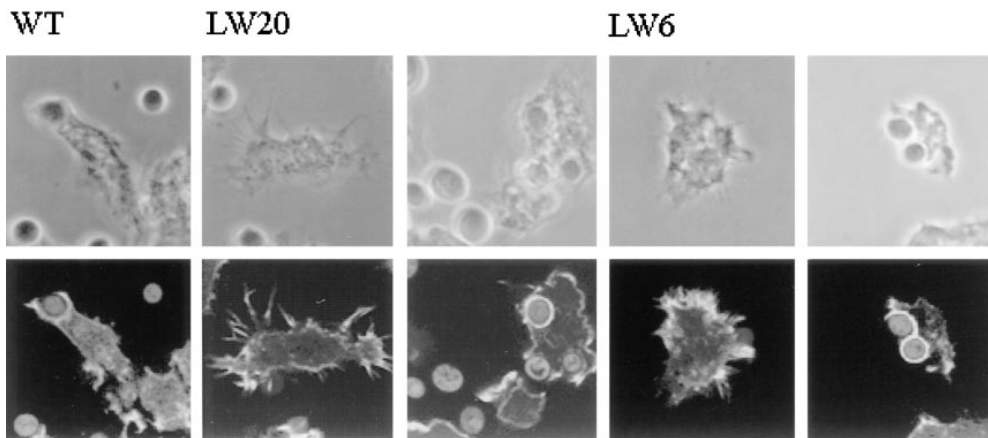

Figure 5. Dynamics of yeast particle uptake by wild type and β subunit–null cells. Serial light microscopy images of AX2 or LW6 cells incubated on a solid substratum with yeast particles. A total of 10^6 WT (*AX2*) or $g\beta^-$ (*LW6*) cells in 5 ml of Soerensen phosphate buffer, pH 6.0, were incubated with 10^7 heat-killed yeast particles in 60-mm Petriperm dishes. Phagocytosis by single cells was followed for 2 h by time-lapse videomicroscopy on a Zeiss Axiovert 35 microscope equipped with a 100× Neofluar objective and a Zeiss ZVS-47DE charge-coupled device videocamera connected to a Panasonic 6050 videorecorder. Images were recorded at 0.5-s intervals. Selected images were captured with the Apple video player and mounted using Adobe Photoshop. Numbers indicate time in s.

Figure 6. Actin localization in wild-type and β subunit–null cells during phagocytosis of yeast particles. WT (*AX2*), rescue (*LW20*) and *gβ⁻* (*LW6*) cells incubated with TRITC-labeled yeast particles on glass coverslip. Phase-contrast and corresponding FITC-phalloidin fluorescence images are shown on alternate lines. For LW20 and LW6, single cells showing membrane projections enriched with actin are shown in addition to cells engulfing yeasts. Cells were incubated with yeast particles on a glass coverslip for 30 min followed by fixation and labeling with FITC-phalloidin.

intracellular Ca^{2+} chelator BAPTA-AM. Interestingly, U73122 interferes with G protein–dependent activation of PLC (Smith et al., 1990) and inhibits IP3-induced mobilization of Ca^{2+} (Willems et al., 1994; Schaloske et al., 1995). Manoalide inhibits primarily PLA2, but several other PLA2 inhibitors, active in *Dictyostelium* (Schaloske and Malchow, 1997), were ineffective, suggesting that PLC is the target of the observed inhibitory effect. Mobilization of intracellular Ca^{2+}, but not Ca^{2+} influx, seems to also be required for efficient phagocytosis, not however via activation of PKC. Neither genistein nor wortmannin or LY294002 affected phagocytosis, which question the involvement of protein tyrosine or PI3 kinases in the process. Consistent with results obtained with the PKA inhibitors, mutants defective in activation of adenylyl cyclase or PKA, or mutants expressing constitutively PKA, showed normal rates of phagocytosis (not shown). It is worth mentioning that none of the drugs at the maximal concentration tested interfered with random cell motility or with stream formation during aggregation (data not shown). In contrast, inhibitors of phosphotyrosine phosphatases, such as phenylarsine oxide or benzylphosphonic acid-$(AM)_2$, inhibited phagocytosis at concentrations that correlated with rounding up of the cells (data not shown).

Discussion

G Protein Controls an Early Step in Phagocytic Uptake

Deletion of the unique G protein β subunit in *Dictyostelium* generates a cell that lacks functional heterotrimeric G proteins. This leads to defects in multiple chemoattractant-induced responses, and, as reported here, in phagocytosis. The β subunit mutation affects an early step of the phagocytic uptake, as evidenced by the strongly reduced efficiency of individual cells in forming phagocytic cups and phagosomes around yeast particles, and by the finding that the initial rate of phagocytosis in shaken suspension is reduced. These results indicate an involvement of the heterotrimeric G protein in particle uptake, which is distinct from its potential role in intracellular phagosome–endosome fusion suggested for macrophages (Desjardins et al., 1994; Béron et al., 1995). The phenotype of the *gβ⁻* mutant differs also in many respects from *Dictyostelium* phagocytosis mutants previously described by us and others. Mutants defective in particle adhesion (Vogel et al., 1980; Ceccarelli and Bozzaro, 1992; Cohen et al., 1994) or talin-null mutants (Niewöhner et al., 1997) fail to phagocytose in shaken cultures but do so on bacterial lawns. In contrast, *gβ⁻* cells are impaired both under shaking conditions and on a solid substratum. Unlike phagocytosis mutants with defects in F-actin cross-linking proteins (Rivero et al., 1996; Cox et al., 1996), the *gβ⁻* mutant does not display their pleiotropic defects in cell–substratum adhesion, locomotion, or cytokinesis. This also distinguishes the β subunit deficiency from elimination of coronin, which has been suggested to lay downstream of heterotrimeric G protein and to act as an integrator of incoming signals to the cytoskeleton (Gerisch et al., 1995; Maniak et al., 1995).

G Protein Regulates the Actin Cytoskeleton during Phagocytosis

We have failed to detect differences between wild-type and *gβ⁻* cells in cell adhesion to a substrate surface, in motility or in spontaneous actin accumulation to leading edges or other sites of the membrane. This indicates that rapid reorganization of the actin cytoskeleton is not impaired in β subunit–null cells.

The *gβ⁻* cells, and to a varying degree the β subunit point mutants, fail to undergo rapid, transient actin assembly upon stimulation with cAMP or bacterial chemoattractants. This impaired actin response is correlated with the phagocytosis defect, suggesting that the G protein is involved in regulating the actin cytoskeleton during phagocytosis. The results with GFP-actin are interesting, in this context, with respect to three questions: (*a*) they show that spontaneous actin accumulation at leading edges or other membrane extensions is not defective in the mutant, and this is consistent with the absence of a general defect in adhesion to substrate, fluid-phase endocytosis, or cytokinesis; (*b*) they further show that cell contact with a yeast par-
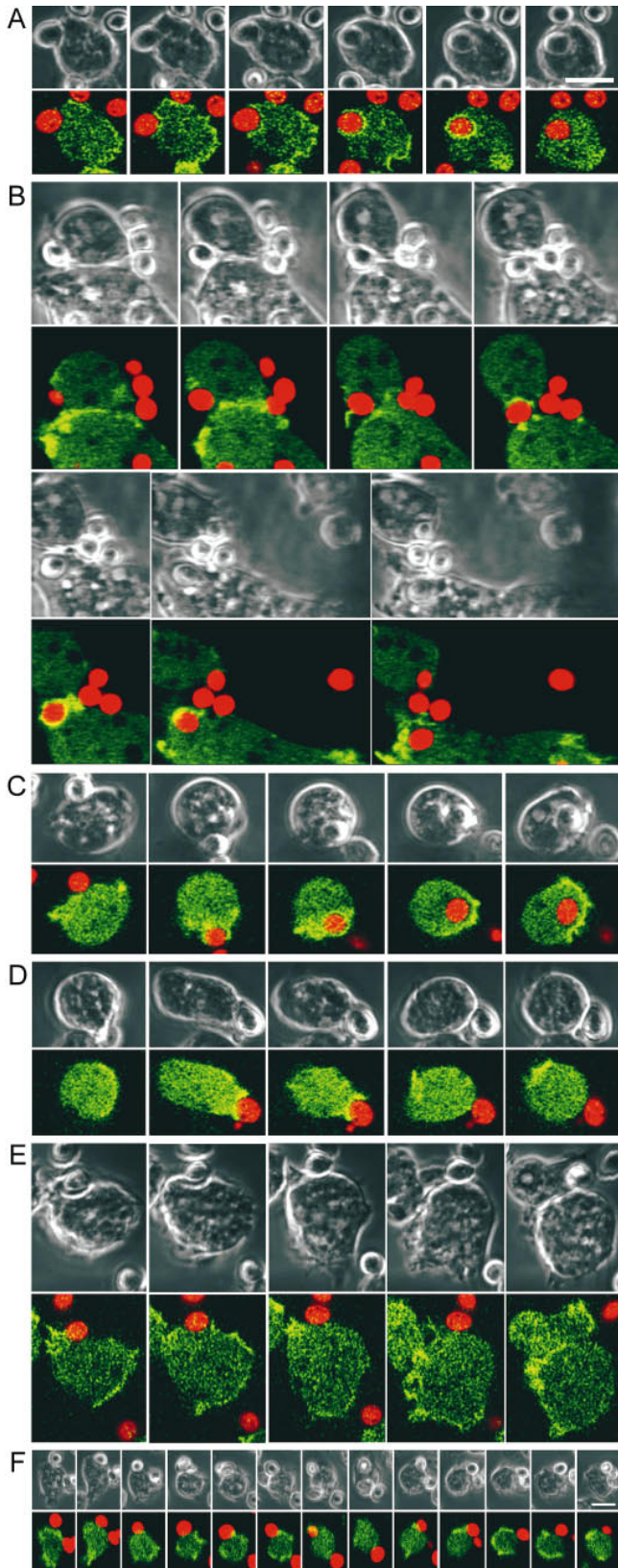
Strain	Adhesion events	(I) GFP–actin enriched at cell–yeast adhesion sites	(II) Particle engulfment	Engulfment rate
				%
WT	53	31	13	42
$g\beta^-$	65	38	3*	8

The number of adhesion events observed for WT (AX2) or $g\beta^-$ (LW6) is shown, in which (I) actin accumulated or was found enriched at cell–yeast adhesion sites and (II) yeast uptake followed. Experimental conditions were as in Fig. 7. *, $P = 0.0013$ relative to WT (Fisher test).

ticle does not automatically trigger local actin assembly, neither in wild-type nor in the mutant. Actin accumulation occurs only in ~50% of the adhesion events with no differences between wild-type and mutant; and (c) they finally show that the $g\beta^-$ cells, even when actin is enriched at cell–yeast adhesion sites, are strongly inhibited in their ability to reshape the actin meshwork into a phagocytic cup, and eventually a phagosome.

We thus propose that a G protein–linked process regulates an appropriate actin assembly beneath the plasma membrane leading to phagocytic cup and phagosome formation. Some evidence suggests that phagosome formation requires a different cytoskeletal organization as, for example, cell spreading (Cannon and Swanson, 1992). G protein–linked signal transduction may be required for this reorganization as occurs for actin assembly in chemotactically-induced pseudopods.

Cross-Talk between Chemotactic and Phagocytic Stimuli

There are multiple chemoattractant receptors and Gα subunits in *Dictyostelium* that are responsible for processing a variety of chemotactic stimuli (Parent and Devreotes, 1996). Double deletion of the chemoattractant receptors, cAR1 and cAR3, or of the α subunit Gα2 linked to these receptors, blocked responses to the chemoattractant cAMP, and deletion of the Gα4 subunit blocked responses to folic acid, but none of these mutations eliminated the chemo-

Figure 7. Phagocytosis and actin dynamics in GFP–actin-transfected wild-type (*A* and *B*) and β-null (*C–F*) cells. Each panel (*A–F*) shows a series of images recorded at intervals of 34 s. Phase-contrast and corresponding GFP–actin fluorescence images are shown on alternate rows. In the fluorescence images, TRITC-labeled yeast particles are shown in red, whereas increas-

ing intensities of GFP–actin are pseudocolored from dark green to light yellow. *A–C* show successful phagocytosis in AX2 (*A*), AX3 (*B*), and LW6 (*C*). In all cases, an actin-enriched layer surrounds the particle during uptake and disappears upon engulfment. In *B,* two cells compete for a particle at the left-hand side of the frames. The particle is first attached to the cell on top, and induces a rim of accumulated actin (*fourth panel*). Simultaneously, the cell on the bottom forms a phagocytic cup and within half a minute succeeds in enclosing the particle, forming a continuous rim of actin. Afterwards, the rim disassembles, beginning at the proximal side of the phagosome, while a new actin-rich leading edge is formed at the extreme right end of the cell (*sixth and seventh panels*). *D–F* illustrate $g\beta^-$ cells that fail to incorporate attached particles. (*D*) A half cup enriched with actin is formed, followed by actin disassembly and detachment of the particle. (*E*) Actin-rich protrusions of the cell are formed to the left and right of an attached particle, but no phagocytic cup is formed. (*F*) A particle adheres to the cell over a period of 7 min without being taken up. Bars, 10 µm.

Table IV. Summary of Drug Effects on Phagocytosis

Drug (IC$_{50}$ μM)	Target	Concentration	Phagocytosis rate (% of control)
Genistein (50)	TK	250 μM	100 ± 5
Staurosporin (.007/.0007)	PKA/PKC	1 μM	108 ± 4
Wortmannin (.005)	PI3K/PI4K	1 μM	85 ± 15
LY294002 (1.4)	PI3K	100 μM	105 ± 2
Isotetrandrine (10)	PLA2	30 μM	100
Aristolochic acid (40)	PLA2	50 μM	103 ± 2
ONO RS082 (7)	PLA2	3.5 μM	80 ± 10
PACOCF3 (15)	PLA2	20 μM	100 ± 10
Calphostin (.05)	PKC	0.05 μM	110 ± 5
Bisindolylmaleimide (.01)	PKC	20 μM	105 ± 2
*Manoalide (.2/1.5)	PLA2/PLC	40 μM	2 ± 2
		9 μM	50
*U73122 (2)	PLC	25 μM	4 ± 2
		8 μM	50
U73343 (inactive analog)		25 μM	85
Okadaic acid (.001/.015)	PP2A, PP1	0.3 μM	98 ± 3
*BAPTA-AM	Ca^{2+}	300 μM	61 ± 2
EDTA	Ca^{2+}/Mg^{2+}	10 μM	90 ± 5
EGTA	Ca^{2+}	10 μM	110 ± 10

AX2 cells were preincubated for 15 min in the cold with each drug at the indicated concentrations followed by addition of 1 vol of FITC-labeled bacteria and further incubation for 15 min at 23°C. The mean values of two duplicate experiments and the variation are shown. Control: AX2 in Soerensen phosphate buffer, containing when required the same amount of DMSO. The IC$_{50}$ values are those reported in the literature or provided by the supplier, and refer to in vitro assays or to activity in mammalian cells. *, drugs with inhibitory activity. Drugs were dissolved in DMSO, except manoalide which was dissolved in ethanol. The final dilution of DMSO varied between 120- and 2,000-fold. Phagocytosis was not affected by DMSO at dilutions above 150-, but was inhibited by 20–30% at a dilution of 100-fold. *TK*, tyrosine kinase; *PKA*, protein kinase A; *PKC*, protein kinase C; *PI3K, PI4K, PI3*, or *PI4* kinase; *PLA2*: phospholipase A2; *PLC*, phospholipase C; *PP2A, PP1*: phospho-protein phophatases 2A and 1.

tactic responses to bacteria-conditioned medium nor did they affect phagocytosis (data not shown). We have also not observed smaller plaques that would suggest a defect in phagocytosis in single null mutants of any of the α subunits (Gα6 has not been examined), nor did we find reduced phagocytosis rates in Gα2 and Gα4 null mutants. It is possible that the α subunits act redundantly in transducing these responses, which would make it difficult to recognize potential receptors required for phagocytosis.

Nevertheless, our results indicate that regulation of the actin cytoskeleton is a common feature in processing chemotactic and phagocytic stimuli, which are both transduced by the G protein β subunit. This is consistent with the finding that phagocytic and chemotactic stimuli compete in recruiting coronin and actin-binding proteins (Maniak et al.,1995). In contrast to chemotaxis, however, which is completely blocked in gβ⁻ cells, phagocytosis is only partially inhibited in these cells. This may suggest either the existence of a G protein–independent pathway mediating phagocytosis or that the G protein acts at different levels in regulating the actin cytoskeleton in chemotaxis or phagocytosis.

Chemotaxis and phagocytosis in *Dictyostelium* exhibit a major distinct feature that also points to a different regulation of actin polymerization, or of cytoskeletal reorganization, by the β subunit. Local chemotactic stimuli trigger pseudopod formation quite automatically and lead to chemotactic locomotion, as long as the stimulus persists.

In contrast, cell contact with a yeast particle does not always induce local membrane extensions to form a phagocytic cup. In addition, despite prolonged attachment of a yeast particle to the cell surface, or even formation of a phagocytic cup, the phagocytic process remains reversible, as shown by Maniak et al. (1995), who have provided evidence in support of a zipper mechanism (Swanson and Baer, 1995) for phagocytosis in *Dictyostelium.* The present results further confirm these observations. It is, however, possible that yeast particle uptake might differ in some important aspects from bacterial uptake, thus some caution is required in extending these conclusions to phagocytosis of bacteria.

The preliminary finding that both the intracellular Ca^{2+} chelator BAPTA-AM and U73122, a specific inhibitor of receptor-stimulated PLC in neutrophils (Smith et al., 1990) blocked phagocytosis suggests a role for IP3 and Ca^{2+} in this process, and raises the possibility that the defect in the β subunit–null cells could be linked to the inability to activate PLC. To confirm this hypothesis it will be necessary to determine which step in phagocytosis is blocked upon cell treatment with these drugs. We cannot exclude that these inhibitors affect the phagocytosis rate indirectly, by interfering with intracellular processes, such as phagosome–endosome fusion or receptor recycling, whereas we have shown that the β subunit–null cells are blocked in actin reorganization in the phagocytic cup. Interestingly, the same inhibitors did not significantly influence chemotactic motility during aggregation (data not shown), suggesting that downstream pathways leading to phagocytosis and chemotaxis might be partially different.

Activation Mechanisms of the Gβ Subunit

A G protein–dependent step in particle engulfment raises a question: what are the signals for G protein–linked actin reorganization during phagocytic cup formation? The correlation found between chemoattractant-stimulated F-actin formation and phagocytosis points to a common role for the G protein in regulating the actin cytoskeleton in chemotaxis and phagocytosis, but is no evidence that chemotactic stimuli are the triggering signals for phagocytosis. With regard to latex beads, whose uptake is decreased in gβ⁻ cells and rescued by expression of the β subunit, the possibility of chemoattractants that may be released from bacteria is excluded. The impaired uptake of heat-killed yeast particles by gβ⁻ cells also makes this hypothesis unlikely.

There are in principle three possibilities: (*a*) autocrine chemokines may exist in *Dictyostelium*, which are secreted upon particle binding and stimulate G protein–mediated actin reorganization; (*b*) the G protein, or its β subunit, could be activated in response to particle binding to yet unknown receptors; and (*c*) the β subunit might have an integrator function in intracellular propagation of signals arising from the site of initial particle attachment, and this function might be independent of any interactions of G proteins with specific cell-surface receptors. Activation could occur through a clustering effect resulting, for example, from the local geometry of adhesion between cell and particle, as proposed for syk tyrosine kinase involvement in phagocytosis (Greenberg et al., 1996). The correlation found between phagocytosis and chemoattractant-stimu-

lated actin assembly, as well as the mutual competition between phagocytic cups and leading edges described by Maniak et al. (1995), support the notion that the β subunit of the heterotrimeric G protein converts signals originating from different processes into activities of the cytoskeleton.

References

Allen L.A., and A. Aderem. 1996. Mechanisms of phagocytosis. *Curr. Opin. Immunol.* 8:36–40.

Aubry, L., G. Klein, J. Martiel, and M. Satre. 1993. Kinetics of endosomal pH evolution in *Dictyostelium discoideum. J. Cell Sci.* 105:861–866.

Beròn, W., M.I. Colombo, L. Mayorga, and P.D. Stahl. 1995. In vitro reconstitution of phagosome-endosome fusion: evidence for regulation by heterotrimeric GTPases. *Arch. Biochem. Biophys.* 317:337–342.

Bozzaro, S., and G. Gerisch. 1978. Contact sites in aggregating cells of *Polysphondylium pallidum. J. Mol. Biol.* 120:265–280.

Bozzaro, S., and E. Ponte. 1995. Cell adhesion in the life cycle of *Dictyostelium. Experientia.* 51:1175–1188.

Bozzaro, S., R. Merkl, and G. Gerisch. 1987. Cell adhesion: its quantification, assay of the molecules involved, and selection of defective mutants in *Dictyostelium* and *Polysphondylium. Methods Cell Biol.* 28:359–385.

Cannon, G.J., and J.A. Swanson. 1992. The macrophage capacity for phagocytosis. *J. Cell Sci.* 101:907–913.

Ceccarelli, A., and S. Bozzaro. 1992. Selection of mutants defective in binding to immobilized carbohydrates in *Dictyostelium discoideum. Anim. Biol.* 1:59–68.

Chia, C.P. 1996. A 130-kDa plasma membrane glycoprotein involved in *Dictyostelium* phagocytosis. *Exp. Cell Res.* 227:182–189.

Cohen, C.J., R. Bacon, M. Clarke, K. Joiner, and I. Mellman. 1994. *Dictyostelium discoideum* mutants with conditional defects in phagocytosis. *J. Cell Biol.* 126:955–966.

Cox, D., D. Wessels, D.R. Soll, J. Hartwig, and J. Condeelis. 1996. Re-expression of ABP-120 rescues cytoskeletal motility, and phagocytosis defects of ABP-120− *Dictyostelium* mutants. *Mol. Biol. Cell.* 7:803–823.

Desjardins, M., J.E. Celis, G. Van Meer, H. Dieplinger, A. Jahraus, G. Griffiths, and L.A. Huber. 1994. Molecular characterization of phagosomes. *J. Biol.Chem.* 269:32194–32199.

Devreotes, P.N., and S.H. Zigmond. 1988. Chemotaxis in eukaryotic cells: a focus on leukocytes and *Dictyostelium. Annu. Rev. Cell Biol.* 4:649–686.

Faix J., G. Gerisch, and A.A. Noegel. 1992. Overexpression of the csA cell adhesion molecule under its own cAMP-regulated promoter impairs morphogenesis in *Dictyostelium. J. Cell Sci.* 102: 203–214.

Gerisch, G. 1959. Ein Submerskulturverfahren für entwicklungsphysiologische Untersuchungen an *Dictyostelium discoideum. Naturwissenschaften.* 46:654–656.

Gerisch, G., R. Albrecht, C. Heizer, S. Hodginkson, and M. Maniak. 1995. Chemoattractant-controlled accumulation of coronin at the leading edge of *Dictyostelium* cells monitored using a green fluorescent protein-coronin fusion protein. *Curr. Biol.* 5:1280–1285.

Greenberg, S. 1995. Signal transduction of phagocytosis. *Trends Cell Biol.* 5:93–99.

Greenberg, S., P. Chang, and S.C. Silverstein. 1994. Tyrosine phosphorylation of the gamma subunit of the Fc gamma receptors, p72syk, and paxillin during Fc-receptor mediated phagocytosis in macrophages. *J. Biol. Chem.* 269: 3897–3902.

Greenberg S., P. Chang, D.C. Wang, R. Xavier, and B. Seed. 1996. Clustered syk tyrosine kinase domains trigger phagocytosis. *Proc. Natl. Acad. Sci. USA.* 93:1103–1107.

Hackam D.J., O.D. Rotstein, A. Schreiber, W.J. Zhang, and S. Grinstein. 1997. Rho is required for the initiation of calcium signaling and phagocytosis by Fc gamma receptors in macrophages. *J. Exp. Med.* 186:955–966.

Hall, A.L., A. Schlein, and J. Condeelis. 1988. Relationship of pseudopod extension to chemotactic hormone-induced actin polymeriaztion in amoeboid cells. *J. Cell. Biochem.* 37:285–299.

Hed, J. 1986. Methods for distinguishing ingested from adhering particles. *Methods Enzymol.* 132:198–204.

Humbel, B.M., and E. Biegelmann. 1992. A preparation protocol for postembedding immunoelectron microscopy of *Dictyostelium discoideum* cells with monoclonal antibodies. *Scanning Microsc.* 6:817–825.

Indik, Z.K., J.G. Park, S. Hunter, and A.D. Schreiber. 1995. The molecular dissection of Fc gamma receptor mediated phagocytosis. *Blood.* 86:4389–4399.

Kundra, V., J.A. Escobedo, A. Kazlauskas, H.K. Kim, S.G. Rhee, L.T. Williams, and B.R. Zetter. 1994. Regulation of chemotaxis by the platelet-derived growth factor receptor-beta. *Nature.* 367:474–476.

Lilly, P., L. Wu, D.L. Welker, and P.N. Devreotes. 1993. A G-protein β subunit is essential for *Dictyostelium* development. *Genes Dev.* 7:986–995.

Malchow, D., O. Lüderitz, O. Westphal, G. Gerisch, and V. Riedel. 1967. Polysaccharide in vegetativen und aggregationsreifen Amoeben von *Dictyostelium discoideum.* I. In vivo Degradierung von Bakterien-Lipopolysaccharid. *Eur. J. Biochem.* 2:469–479.

Maniak, M., R. Rauchenberger, R. Albrecht, J. Murphy, and G. Gerisch. 1995. Coronin involved in phagocytosis: dynamics of particle-induced relocalization visualized by a green fluorescent protein tag. *Cell.* 83:915–924.

McRobbie, S.J., and P.C. Newell. 1983. Changes in actin associated with the cytoskeleton following chemotactic stimulation of *Dictyostelium disocideum. Biochem. Biophys. Res. Commun.* 115:351–359.

Metchnikoff, E. 1968 (1905). Immunity in Infective Disease. Johnson Reprint Corp., New York. 591 pp.

Murphy, P.M. 1996. Chemokine receptors: structure, function and role in microbial pathogenesis. *Cytokine Growth Factor Rev.* 7:47–64.

Niewöhner, J., I. Weber, M. Maniak, A. Müller-Taubenberger, and G. Gerisch. 1997. Talin-null cells of *Dictyostelium* are strongly defective in adhesion to particle and substrate surfaces and slightly impaired in cytokinesis. *J. Cell Biol.* 138:349–361.

Parent, C.A., and P.N. Devreotes. 1996. Molecular genetics of signal transduction in *Dictyostelium. Annu. Rev. Biochem.* 65:411–440.

Rabinovitch, M. 1995. Professional and nonprofessional phagocytes: an introduction. *Trends Cell Biol.* 5:85–88.

Rivero, F., B. Koppel, B. Peracino, S. Bozzaro, F. Siegert, C.J. Weijer, M. Schleicher, R. Albrecht and A.A. Noegel, 1996. The role of the cortical cytoskeleton: F-actin crosslinking proteins protect against osmotic stress, ensure cell size, cell shape and motility, and contribute to phagocytosis and development. *J. Cell Sci.* 109:2679–2691.

Schaloske, R., and D. Malchow. 1997. Mechanism of cAMP-induced Ca^{2+} influx in *Dictyostelium:* role of phospholipase A2. *Biochem. J. (Tokyo).* 327:233–238.

Schaloske, R, C. Sordano, S. Bozzaro, and D. Malchow. 1995. Stimulation of calcium influx by platelet activating factor in *Dictyostelium. J. Cell Sci.* 108: 1597–1603.

Smith, R.J., L.M. Sam, J.M. Justen, G.L. Bundy, G.A. Bala, and J.B. Bleasdale. 1990. Receptor-coupled signal transduction in human polymorphonuclear neutrophils: effects of a novel inhibitor of phospholipase C dependent processes on cell responsiveness. *J. Pharmacol. Exp. Ther.* 253:688–697.

Sutoh, K. 1993. A transformation vector for *Dictyostelium discoideum* with a new selectable marker *bsr. Plasmid.* 30:150–154.

Swanson, J.A., and S.C. Baer. 1995. Phagocytosis by zippers and triggers. *Trends Cell Biol.* 5:89–93.

Tardif, M., S. Huang, T. Redmond, D. Safer, M. Pring, and S.H. Zigmond. 1995. Actin polymeriaztion induced by GTPγS in permeabilized neutrophils is induced and maintained by free barbed ends. *J. Biol. Chem.* 270:28075–28083.

Thelen, M., and U. Wirthmueller. 1994. Phospholipases and protein kinases during phagocyte activation. *Curr. Opin. Immunol.* 6:106–112.

Vogel, G. 1987. Endocytosis and recognition mechanisms in *Dictyostelium discoideum. Methods Cell Biol.* 28:129–137.

Vogel, G., L. Thilo, H. Schwarz, and R. Steinhart. 1980. Mechanism of phagocytosis in *Dictyostelium discoideum:* phagocytosis is mediated by different recognition sites as disclosed by mutants with altered phagocytic properties. *J. Cell Biol.* 86:456–465.

Watts, D.J., and J.M. Ashwort. 1972. Growth of mix amoebae of the cellular slime mould *Dictyostelium discoideum. Biochem. J. (Tokyo).* 119:171–174.

Westphal, M., A. Jungbluth, M. Heidecker, B. Muhlbauer, C. Heizer, J.M. Schwartz, G. Marriott, and G. Gerisch. 1997. Microfilament dynamics during cell movement and chemotaxis monitored using a GFP-actin fusion protein. *Curr. Biol.* 7:176–183.

Willems, P.H.G., F.H.M.M. Van de Put, R. Enghersen, R.R. Bosch, H.J.M. van Hoof, and J.J.H.M. de Pont. 1994. The interaction of phospholipase A2 with phospholipid analogues and inhibitors. *J. Biol. Chem.* 265:2657–2664.

Wu, L., R. Valkema, P.J.M. Van Haastert, and P.N. Devreotes. 1995. The G protein β subunit is essential for multiple responses to chemoattractants in *Dictyostelium. J. Cell Biol.* 129:1667–1675.

Zigmond, S.H. 1996. Signal transduction and actin filament organization. *Curr. Opin. Cell Biol.* 8:66–73.